Deprotonation and Dimerization of Maleimide in the Triplet State: A Laser Flash Photolysis Study with Optical and Conductometric Detection

Justus von Sonntag,* Wolfgang Knolle, Sergej Naumov, and Reiner Mehnert[a]

Abstract: The photochemistry of maleimide in aqueous solution is governed by the coexistence of up to three different triplet states, the keto triplet ($\lambda_{max}=$ 250, 330 nm, $\lambda_{min}=290$ nm, $pK_a=4.4\pm 0.1$, $\tau=5$ μs), the deprotonated or enolate triplet ($\lambda_{max}=360$, 260 nm, $\lambda_{min}=$ 320 nm, shoulder at 370–380 nm) and a dimer triplet. This biradical is formed by the addition of the keto triplet to the double bond of a ground state maleimide in competition with electron transfer, ($k_{^3MI+MI}=2.6\times10^9$ dm^3 mol^{-1} s^{-1}). Its spectrum is identical to that of the maleimide H-adduct radical ($\lambda_{max}=$ 370–380 (broad), 255 nm (narrow), $\lambda_{min}=290$ nm) and its lifetime is 110 ns. While protolysis is confined to maleimide and aqueous solutions, the dimer triplet is also found in acetonitrile. Dimer triplet formation is also observed with *N*-ethylmaleimide. Time-resolved conductometry and buffer experiments were used to characterise excited state protolysis. Multi-wavelength "global analysis" of the time profiles allowed the separation of the transient spectra and study of the kinetics of the monomer and dimer triplets. The cyclobutane dimer yield (determined by GC) is independent of maleimide concentration. This indicates that the dimer triplet does not contribute significantly to the initiation of free-radical polymerisation. Time-dependent Hartree–Fock calculations agree with the experimental data and further confirm the proposed mechanisms.

Keywords: dimerization · kinetics · maleimides · photochemistry

Introduction

The photochemistry of maleimides is of considerable interest in the field of copolymerisable photoinitiators.[1][2–7] In addition, the use of maleimides as radiation sensitisers[8] and model compounds for photoactive biomolecules[9] has triggered investigations into the mechanism of formation and reactions of their related free radicals.[5, 7, 10, 11]

Interestingly, the triplet state chemistry of maleimides differs substantially from that of "normal" carbonyl triplet states. For example, both abstract an H atom from alcohols, but maleimide triplet **1** (unsubstituted, HMI*^{3}) adds the H atom at the C=C double bond [reaction (1) in Scheme 1] and this leads exclusively to the H-adduct **2**, while "normal" carbonyls give rise to ketyl radicals. Maleimide ketyl radicals **4** are also known, but they result from a protonation of the radical anion **3** [reaction (3), Scheme 1]. The optical and EPR spectra of **2**, **3** and **4** differ considerably, and this allows definite assignment of the spectra. The radical-anion-derived species are formed upon one-electron reduction of ground-[8] or triplet-state[11] maleimides [reaction (2)].

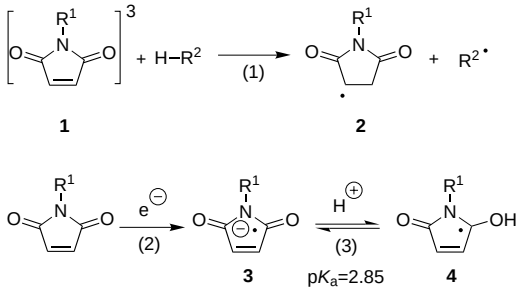

Scheme 1.

N-Substitution perturbs the electronic structure of the maleimide chromophore and, as a consequence, triplet quantum yields vary from unity (maleimide) to negligible (*N*-phenylmaleimide).[9, 12] Moreover, maleimides have a very rich and often unusual photochemistry.[6, 9, 13]

Maleimides show short-lived (<100 ps, a compilation of rate constants is given in Table 1) and, hence, very little fluorescence.[7] The involvement of a triplet state in the photochemistry of maleimides has accordingly been shown in many cases.[4, 5, 7, 9, 11] The UV spectra of HMI*^{3} and of its *N*-alkyl derivatives have been reported.[4, 5, 12] Alkylation at nitrogen red-shifts ground- and triplet-state spectra to a similar extent.

In the present study, the deprotonation of HMI*^{3} is studied in aqueous solution. However, the imide moiety hydrolyses

[a] Dr. J. von Sonntag, Dr. W. Knolle, Dr. S. Naumov, Prof. Dr. R. Mehnert
Institut für Oberflächenmodifizierung IOM e.V.
Permoserstrasse 15, 04318 Leipzig (Germany)
Fax: (+49) 3412-352-584
E-mail: justus@rz.uni-leipzig.de

  0947-6539/02/0818-4199 $ 20.00+.50/0

Table 1. Compilation of rate constants relevant to the present study.

Reaction	Rate constant
6	$0.2 \times 10^6\ s^{-1}$
7	$> 1 \times 10^{10}\ s^{-1}$
8	$2.8 \times 10^6\ s^{-1}$
-8	$7 \times 10^{10}\ dm^3\,mol^{-1}\,s^{-1}$
$9+10$	$2.6 \times 10^9\ dm^3\,mol^{-1}\,s^{-1}$
$11+18$	$9.1 \times 10^6\ s^{-1}$
15	$1.8 \times 10^7\ dm^3\,mol^{-1}\,s^{-1}$

rapidly under even mildly alkaline conditions.[8] This restricts the study to the acidic pH range. Accordingly, the ground-state pK_a of maleimide [equilibrium (4), Scheme 2, pK_a = 10.8 ± 0.2] had been determined in a non-aqueous environment.[14] It will be shown that in aqueous solutions HMI*[3] is an acid with a pK_a of 4.4.

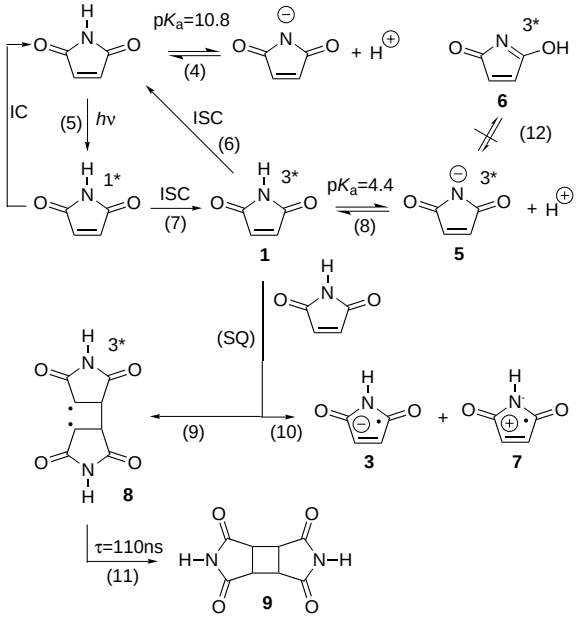

Scheme 2.

Cyclobutane dimer formation is one of the most prominent processes in the photochemistry of electron-deficient olefins.[15] Reactions of the excited species with its own ground state and with an electron-donating partner are known.[15] In maleimide-based systems, cyclobutane dimer formation [reactions (9) and (11) in Scheme 2] is commonly observed with photopolymerisation. It has been suggested that both processes have a common precursor.[16, 17]

In this paper, the spectral and kinetic properties of the triplet precursor of the maleimide cyclobutane dimers will be presented, and it will be shown that the triplet-state dimer is too short-lived to contribute to initiation.

Results and Discussion

Excited state deprotonation

Determination of the pK_a in buffered solutions: The spectra of the intermediates immediately after the excitation of maleimide in aqueous solution depends on the pH (Figure 1). This effect is more pronounced in buffered solution. The change of the optical spectra with pH can thus be used to determine the pK_a of the maleimide triplet.

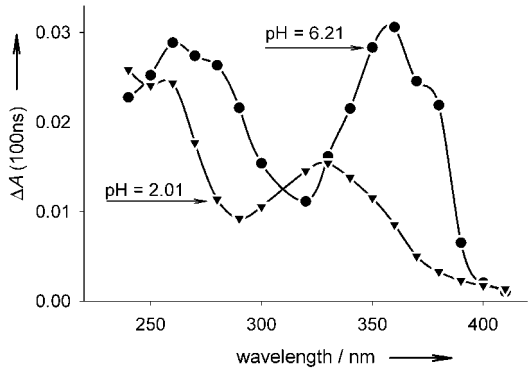

Figure 1. Transient spectra at 100 ns, pH 2.01 (▼) and 6.21 (●). 308 nm laser flash photolysis of maleimide (1.0 mmol dm^{-3}) in nitrogen-degassed phosphate buffer (1 mol dm^{-3}), pH adjusted with perchloric acid or sodium hydroxide, respectively.

The choice of buffer is very limited, since the buffer has to be inert against hydrogen abstraction and electron transfer, and also transparent down to 240 nm. Phosphate-based buffer complies with these requirements, but catalyzes the maleimide hydrolysis at a pH near 7.

In acidic solution, the transient spectrum (Figure 1, ▼) is identical to the primary triplet spectrum, which is known from earlier work.[5, 12] With increasing pH, enolate **5** contributes and finally dominates the spectrum (Figure 1, ●).

Effects of buffer concentration: It is usual practice to use low buffer concentrations in order to minimise impurities. Figure 2 shows the pitfalls that are associated with the settling of equilibria when the object of scrutiny is short-lived. The

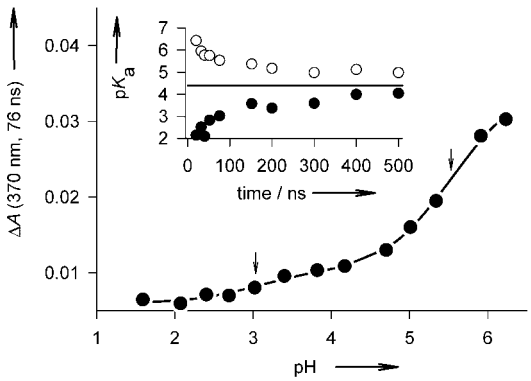

Figure 2. Effect of insufficient buffer concentration on maleimide deprotonation in laser flash photolysis. Maleimide (1.0 mmol dm^{-3}) in nitrogen-purged aqueous phosphate buffer (0.22 mol dm^{-3}). The "titration" curves at 370 nm and different times (only one example (76 ns) is given in the main graph) show two pK_a values (indicated by the arrows in the main graph, given as a function of time in the inset). Solid line (——) in the main graph: fit function with two independent pK_a; solid line in the inset: asymptote with pK_a = 4.4.

0947-6539/02/0818-4200 $ 20.00+.50/0 *Chem. Eur. J.* **2002**, *8*, No. 18

settling of an equilibrium involves bimolecular reactions between the buffer and the transient acid. The rate of these reactions are governed by the product of the pK_a difference and the buffer concentration.[18]

At low buffer concentration, when the pH-dependence of the absorbance is measured shortly after the pulse, two pK_a are observed rather than one. These values converge with time to one value (Figure 2). This effect is caused by the fact that at low buffer concentration and very short time, a larger pK_a difference is required to protonate/deprotonate the transient species. This effect is consistent with the formulae given by Eigen and co-workers,[18] but was not reported at that time. A reliable determination of the pK_a thus requires very high concentrations of phosphate to rapidly buffer the system. At a concentration of 1M phosphate, the equilibrium is reached fast enough and from 100 ns onwards the "titration" curve (Figure 3) becomes well defined, yields a pK_a of 4.4 ± 0.1, and is independent of time and wavelength.

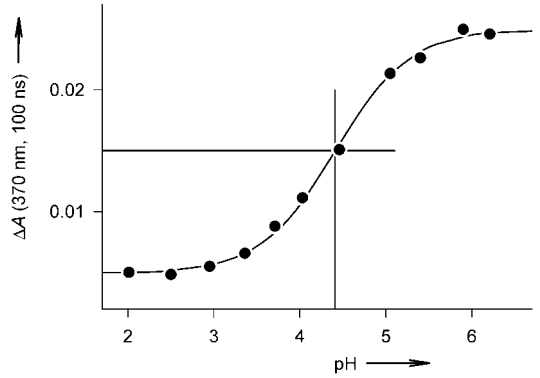

Figure 3. "Titration" curve at 370 nm, 100 ns. p$K_a = 4.4 \pm 0.1$. Solid line: sigmoid fit function with slope fixed to ln(10) as required for a pK_a curve. Experimental conditions as in Figure 1.

In neutral unbuffered solution, the same initial spectrum is found as in acidic solution (in which the species persists), and, hence, we can conclude that the observed pK_a is caused by the deprotonation of HMI^{3*} and not by its protonation, that is, HMI^{3*} is an acid, not a base. At first, it is surprising that an imide deprotonates in its excited state, but it is not uncommon that *N*-H acids behave like *O*-H acids in this respect.[18] This finding will be further substantiated later.

Conductivity detection: The proton has the highest equivalent conductivity of all ions (350×10^{-4} m^2 S mol^{-1}). Hydroxide, OH^-, has a conductivity of 198×10^{-4} m^2 S mol^{-1}, while all organic ions span the narrow range from ≈ 25 to $\approx 55 \times 10^{-4}$ m^2 S mol^{-1} (from large ions, e.g., dodecyl sulfate to very small ions, e.g., formate, respectively).[19] Protolytic reactions can therefore be followed conductometrically and their yields quantified.

When aqueous maleimide is subjected to a laser flash, a strong conductivity signal (Figure 4) builds up which indicates the release of a proton. The usual procedure to check for

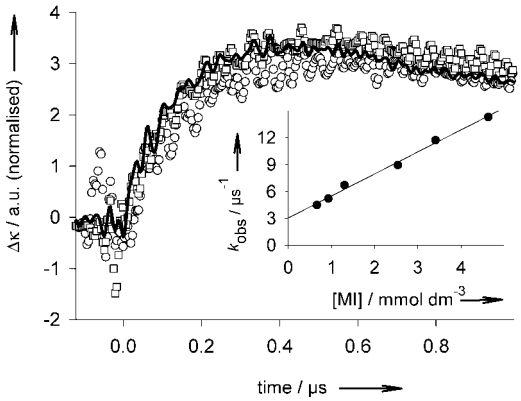

Figure 4. Transient conductivity at three different doses, normalised to dose.[20, 21] A solution of maleimide (1.3 mmol dm^{-3}) in nitrogen-purged water, Fourier filtered to 50 MHz bandwidth. 100% laser intensity (——); 50% intensity (□);25% intensity (○). Inset: observed rate of buildup vs maleimide concentration, $k_{obs} = k_{obs,0} + k_{SQ} = 3.0 \times 10^6\ s^{-1} + 2.6 \times 10^9$ dm^3 mol^{-1} s^{-1}.

deprotonation would be to test whether the signal reverts its sign on increasing the pH from 6 to 9 (at higher pH the released protons would recombine rapidly with OH^- with the net result that the strongly conducting OH^- is substituted by an organic anion). This cannot be applied here because maleimide hydrolyzes too fast at pH > 7.[8]

However, the reverse check can be performed, and no sign reversal is observed on addition of sulfuric acid (∼pH 5); therefore, the conductivity increase is not caused by formation of OH^-.

The signal amplitude (Figure 4) is proportional to the laser intensity (contributions by biphotonic processes are dicussed below), and the rate of conductivity build-up is proportional to the maleimide concentration (Figure 4, inset).

Reactions that compete with the deprotonation of the acidic triplet state increase the observed rate of deprotonation and decrease the proton yield. Two such processes are known, the intrinsic lifetime and the self-quenching [reactions (9) and (11)]. The intrinsic lifetime of triplet maleimide, which is determined below to be $0.2 \times 10^6\ s^{-1}$, contributes with the intrinsic rate of deprotonation to the intercept in the inset of Figure 4, ($k_{obs,0} = 3.0 \times 10^6\ s^{-1}$). Self-quenching causes the slope of the straight line (k_{SQ}). The value of 2.6×10^9 dm^3 mol^{-1} s^{-1} is identical to the value determined by "global analysis" of the optical spectra (vide infra).

Radical ions (especially the radical cation, which probably reacts with water to produce a proton) are formed by self-quenching [reaction (10), Scheme 2] and also cause conductivity.[5]

Quantum yield: A major advantage of conductometric detection is the fact that fully deprotonated acids have the same specific conductivity, since the proton conductivity governs the overall effect and anions of comparable molecular weight also have a similar specific conductivity. The comparison with actinometry (formation of a 2-nitrosobenzoic acid from 2-nitrobenzaldehyde with a quantum yield of 0.5),[22] therefore, leads directly to the quantum yield of deprotonation.

  0947-6539/02/0818-4201 $ 20.00+.50/0

The competition of self-quenching and deprotonation renders the proton quantum yield a function of the maleimide concentration (Figure 5, top). This function can be described

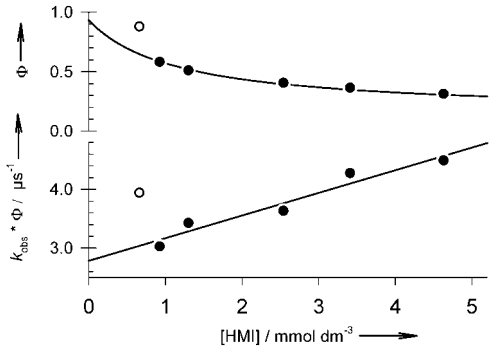

Figure 5. Quantum yield of deprotonation (Φ) vs maleimide concentration (top); product of k_{obs} and Φ vs maleimide concentration (bottom). The solid lines represent the same mathematical formula [Eq(1)]. Experimental conditions as in Figure 4. The intercept is $2.8 \times 10^6\ s^{-1}$, the slope is $3.9 \times 10^8\ dm^3\,mol^{-1}\,s^{-1}$. An outlier (○) has been omitted from regression.

by Equation (1); however, this equation is so ill-conditioned that the acquired data are not sufficiently precise to allow nonlinear curve fitting.

$$\Phi = \frac{\Phi_{\text{deprotonation}}\, k_{\text{deprotonation}} + \Phi_{\text{radical ion}}\, k_{SQ}\,[\text{HMI}]}{k_{\text{deprotonation}} + k_{\text{intrinsic}} + k_{SQ}\,[\text{HMI}]} \quad (1)$$

The denominator in Equation (1) is equal to k_{obs} ($k_{obs} = k_{\text{deprotonation}} + k_{\text{intrinsic}} + k_{SQ} \cdot [\text{HMI}] = 3.0 \times 10^6\ s^{-1} + 2.6 \times 10^9\ dm^3\,mol^{-1}\,s^{-1}\,[\text{HMI}]$). As k_{obs} is independently accessible from the time profiles, a modified equation is derived [Eq. (2)]. The plot of the product of quantum yield and k_{obs} (which is determined for each data point) versus maleimide concentration yields a straight line (Figure 5, bottom).

$$k_{obs}\,\Phi = \Phi_{\text{deprotonation}}\, k_{\text{deprotonation}} + \Phi_{\text{radical ion}}\, k_{SQ}\,[\text{HMI}] \quad (2)$$

The data can now be subjected to reliable linear regression. The quantum yield of radical ions calculated from the slope ($\Phi\, k_{obs} = 3.9 \times 10^8\ dm^3\,mol^{-1}\,s^{-1}$) and the rate of self-quenching ($k_{SQ} = 2.6 \times 10^9\ dm^3\,mol^{-1}\,s^{-1}$) is 0.15. This value is comparable to that of 0.1 given in reference [12] and the value of 0.12 deduced from trapping the maleimide radical anion by tetranitromethane (calculated from ε(HMI^{3*}, 330 nm) = $300\ m^2\,mol^{-1}$[12] and ε(nitroform anion, 350 nm) = $1500\ m^2\,mol^{-1}$;[23] data not shown).

The product of triplet quantum yield[24] and rate of deprotonation ($2.8 \times 10^6\ s^{-1}$) is somewhat smaller than the value of $3.0 \times 10^6\ s^{-1}$ that was determined from the intercept in Figure 4, inset. This has two implications. On one hand, the quantum yield cannot be less than the ratio of these two values, that is, 93%, if the intrinsic lifetime of the HMI^{3*} is infinite. On the other hand, any finite intrinsic lifetime adds to the rate at vanishing maleimide concentration. Parallel (pseudo) first-order reactions lead to an observed rate that is equal to the sum of the two rates. The maximum rate of the intrinsic triplet decay is, therefore, $0.2 \times 10^6\ s^{-1}$, if a quantum yield of unity is assumed. This is noticeably slower than the value of $1.3 \times 10^6\ s^{-1}$ ($\tau = 770$ ns) from earlier work.[5] The reasons for this will be discussed below in the context of dimer formation.

The rate of deprotonation is in any case in the range of $2.8 - 3.0 \times 10^6\ s^{-1}$. Eigen and co-workers established the rule that the protonation of an anion in water is very close to diffusion controlled.[18] The rate constants vary from 1×10^{10} for bulky organic anions to $8 \times 10^{10}\ dm^3\,mol^{-1}\,s^{-1}$ for HS^-.[18] A pK_a of 4.4 is therefore equivalent to a rate of deprotonation of $0.3 - 4 \times 10^6\ s^{-1}$; the value of $2.8 - 3.0 \times 10^6\ s^{-1}$, determined above, fits well into this range.

Isotope effect: Dedeuteronation is slower than deprotonation. The ratio of the rates of deprotonation to dedeuteronation depends on the pK_a; for an acid with a pK_a of 4.4, a kinetic isotope effect close to 3 is expected[25]. This is found experimentally.

N-*Alkylmaleimides*: Laser photolysis of *N*-alkylmaleimides gives rise to a negligible build-up of conductivity which is just sufficient to account for the formation of radical ions upon self-quenching ($\Phi \approx 0.01$).[5, 7, 12]

Quantum chemical calculations: The success of quantum chemical calculations in predicting the EPR spectra of maleimide-derived transients (e.g., the radical anion **3**)[7] suggests that the calculated geometry is reliable. Calculated optical spectra, however, used to be of dubious value. However, the modern time-dependent Hartree–Fock (TDHF) method reproduces at least qualitatively the experimental spectra so that we include them here to further support our assignment (Table 2).

Assuming an equivalent rate of protonation for the carbonyls [reaction (−12), Scheme 3] and the nitrogen [reaction (−8)], protonation of the triplet enolate **5** should lead to a 2:1 distribution of the two triplet species **6** and **1**.

Table 2. Calculated electronic spectra.[a]

Molecule (No.)	λ [nm] exptl	oscillator calcd	strength
HMI^{3*} (**1**)	250	279	0.128
	330	317	0.126
HMI-H (**2**)	255	277	0.006
	370	330	0.065
HMI$^-$ (**3**)	260	215	0.153
	330	265	0.013
	420	386	0.184
MI3^{*-} (**5**)	270	298	0.018
	360	383	0.185
	380	490	0.019
HMI-HMI^{3*} (**8**)	255	274	0.011
		324	0.005
	370	326	0.140
$^{3-}$MI-HMI (N → C) (**10**$^{*-}$)	< 240	313	0.065
	330	394	0.170
$^{3-}$MI-HMI (C → C)	< 240	410	0.053
	330	332	0.045
FMI$^-$ (**12**)	< 240	256	0.014
	330	387	0.242

[a] Method used: Time dependent Hartree–Fock (TD-HF) using B3LYP/6—31G(d) optimised molecular geometries taking the solvent (water) into account by employing the Onsager (SCRF = dipole) model.

0947-6539/02/0818-4202 $ 20.00+.50/0 *Chem. Eur. J.* **2002**, *8*, No. 18

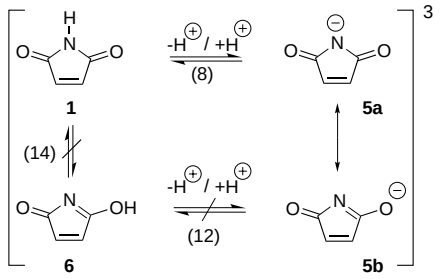

Scheme 3.

However, we have not found any experimental evidence for the existence of the triplet enol **6**. Presumably, the bona-fide assumption of equivalent rates of protonation does not hold, and this is consistent with the quantum chemical calculations, which show a decisively higher spin density on the nitrogen (mesomeric dominance of **5a**).

Sensitisation

Triplet acetone has a high triplet energy and a well-known lifetime and spectrum.[26] Apart from its ground-state spectrum, which obscures the region below 300 nm, acetone is a good triplet sensitiser. Triplet sensitisation is used to substantiate the theory that these phenomena are caused by the triplet state. Laser photolysis of aqueous acetone solutions (0.17 mol dm^{-3}) in the presence of maleimide (Figure 6) leads to the same pH dependence of the transient spectra as shown in Figure 1.

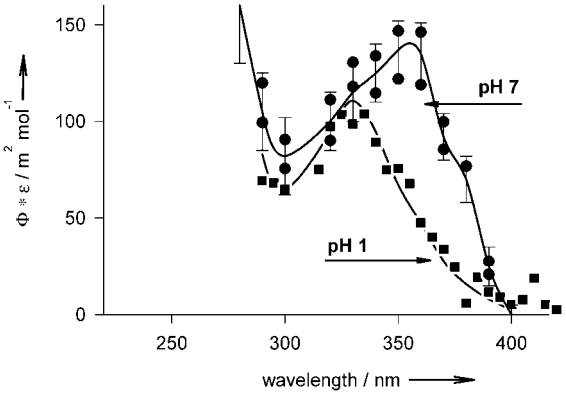

Figure 6. Acetone (0.17 mol dm^{-3}) sensitised triplet spectrum of maleimide in N_2-purged aqueous solution. 6.5×10^{-5} mol dm^{-3} maleimide at pH 7 (●); 12×10^{-5} mol dm^{-3} maleimide at pH 1 (H_2SO_4) (■). For ease of comparison with Figure 1 the same wavelength range was used.

Sensitised conductivity increase: The rate of increase of conductivity is not linear with maleimide concentration, but shows a saturation-type behaviour (Figure 7). The observed rate can be modelled by the harmonic mean of the rates of the individual reactions [Eq. (3)]. This function is derived from the observation that the shape of a sequential formation cannot be resolved when the starting point of the reaction is smeared by a finite pulse width (and further obscured by the electromagnetic noise of the laser). The data are fitted with a simple first-order buildup and the result subjected to Equation (3) to extract the relevant time constants, that is, the rates of energy transfer (ET), the unimolecular deprotonation reaction (0) and the self-quenching (SQ). A discussion of the mathematics behind this is beyond the scope of this paper, but will be published separately.

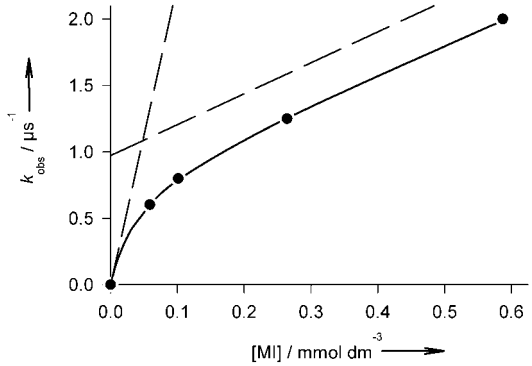

Figure 7. Rate of conductivity buildup caused by maleimide when sensitised with triplet acetone (0.17 mol dm^{-3} acetone in nitrogen-purged water, different maleimide concentrations). ——: Fit function according to Equation (3); - - - -: Asymptotes. Note that the calculated asymptote for the slower reaction differs from an eye-ball fit in the intercept.

$$k_{obs} = \frac{k_{ET}[MI](k_0 + k_{SQ}[MI])}{k_{ET} + k_0 + k_{SQ}[MI]} \quad (3)$$

The values obtained from the fit agree with expectation: the energy transfer (2.2×10^{10} dm^{3}mol^{-1}s^{-1}) is practically diffusion controlled, the rate constants of deprotonation (1×10^6 s^{-1}) and self-quenching (2.3×10^9 dm^{3}mol^{-1}s^{-1}) are close to those values determined above.

Biphotonic excitation: The use of a high photon-flux excitation source may lead to biphotonic excitation. In this case, this is especially favoured by the absorption coefficient, $\varepsilon_{308\,nm}$, of the maleimide triplet state (230 m^{2}mol^{-1}), which is ten times larger than that of its ground state (22 m^{2}mol^{-1}),[12, 21] and a triplet quantum yield of unity.[12]

The biphotonic process shows a much faster buildup of transient conductivity than the monophotonic excitation (Figure 8). The rate of increase (indicating a p$K_a < 2$) is too close to the detection limit of the experiment to be quantified, but is slow enough to exclude photoionisation. Another, more stringent proof of the absence of photoionisation is the lack of any trace of the solvated electron ($\varepsilon_{max} = 1900$ m^{2}mol^{-1} at 720 nm)[27] in transient spectra measured with the same setup.

The pK_a of ground state maleimide (10.8) is much higher than that of its lowest excited triplet state (4.4). Thus it is not surprising that an even higher excited triplet state should be even more acidic (p$K_a < 2$).

Reactions of the enolate triplet: The results of quantum chemical calculations on the triplet enolate suggest that this molecule attacks another maleimide molecule and attaches the nitrogen atom to the double bond of a ground state molecule [reaction (13) in Scheme 4] in similar manner to the radical cation attack suggested in reference [28]. The product

  0947-6539/02/0818-4203 $ 20.00+.50/0

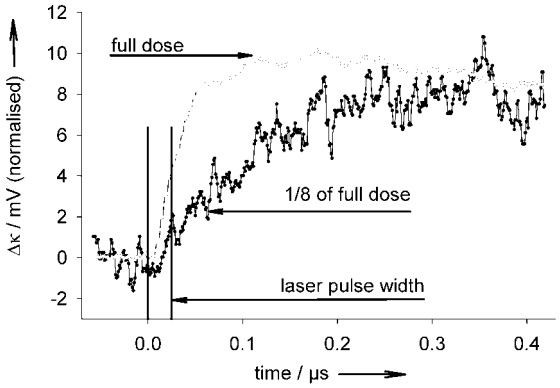

Figure 8. Biphotonic conductivity buildup of photoexcited maleimide (2.8 mmol dm^{-3}) in argon-purged water. The upper curve (high dose) shows biphotonic behaviour (fast deprotonation), while the lower curve (small dose) corresponds to the data shown in Figure 4. Data obtained at intermediate doses are omitted for clarity.

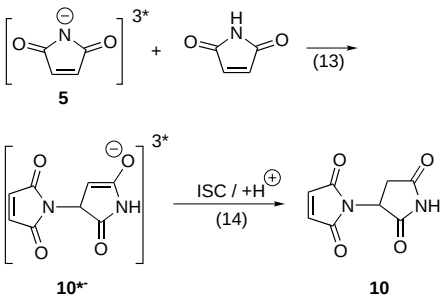

Scheme 4.

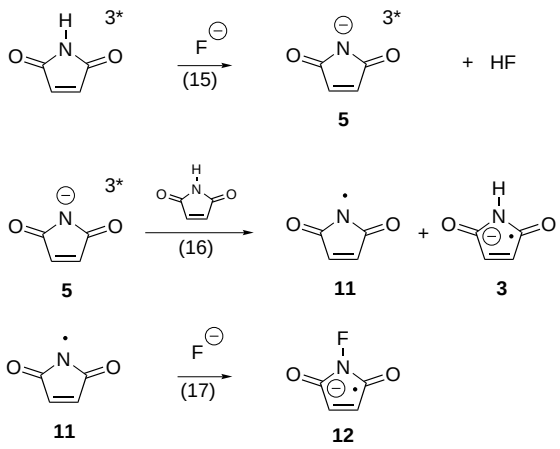

Scheme 5.

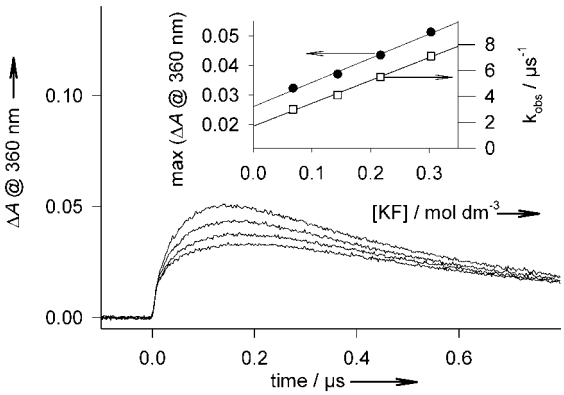

Figure 9. Maleimide (1.12 mmol dm^{-3}) excited state protolysis catalyzed by various fluoride concentrations (cf. inset), pH 7, nitrogen-purged. Inset: yield at maximum (●) and k_{obs} (□) vs fluoride concentration.

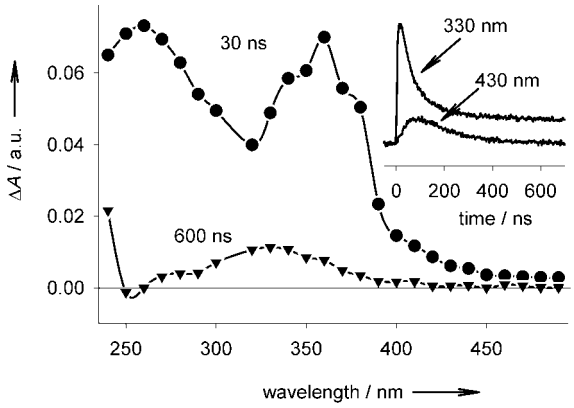

Figure 10. Transient spectra obtained from laser photolysis of maleimide (0.01 mol dm^{-3}) in fluoride buffer(1 mol dm^{-3}), nitrogen-purged.

of reactions (13) and (14) (in Scheme 4), the *N*-succinimidylmaleimide **10**, differs from the cyclobutane dimer **9**.

This reaction can only be investigated at high maleimide and molar buffer concentrations. Phosphate catalyses the hydrolysis at higher pH, therefore, a different buffer is required for this experiment.

Fluoride as buffer: Fluoride is very rarely used as a buffer, since it can be only used at neutral pH as hydrofluoric acid is not only toxic but also corrodes the glassware. We first used fluoride as a buffer while measuring the rates of reaction of halides with triplet maleimide.[5] Fluoride has the advantage that on addition to a neutral aqueous solution it does not perturb the pH and that, in contrast phosphate at pH 7, it does not catalyze the hydrolysis of ground-state maleimide.

Hydrofluoric acid has a pK_a of 3.45.[29] The equilibrium between keto triplet **1** + F^- and HF + triplet enolate **5** [reaction (15), Scheme 5] lies toward the left side. This is reflected in the slow rate of fluoride catalysis of triplet maleimide deprotonation ($k = 1.8 \times 10^7$ dm^3 mol^{-1} s^{-1}, Figure 9, inset).

The transient spectrum within the pulse train in Figure 10 is again similar to that of the enolate but has a contribution from a longer lived transient. The delayed increase typical of the formation of the maleimide triplet dimer **8** is found, but another transient species is also detected. This can either be attributed to the triplet *N*-succinimidylmaleimide **10** or alternatively to the *N*-fluoromaleimide radical anion **12**, a product of the reaction of the maleimide enolyl radical **11** with fluoride [reaction (17), Scheme 5].

This last assignment is based on the chemistry of *N*-bromosuccinimide, in which the succinimide-ring is such a

0947-6539/02/0818-4204 $ 20.00+.50/0 *Chem. Eur. J.* **2002**, *8*, No. 18

strong electron acceptor that the radical anion expels a bromine atom.[30]

Dimerisation

Non-aqueous inert solvents (acetonitrile): The excited-state deprotonation discussed above does not take place in acetonitrile; thus, one complication is eliminated. A satisfactory signal strength, however, requires at least millimolar concentrations of maleimide (or higher, in the case of the *N*-substituted malemides due to their low triplet state quantum yield[12]). Under these conditions, the reaction of ground-state maleimide with the triplet-state maleimide ($k = 1.6 \times 10^9$ dm^3 mol^{-1} s^{-1};[5], $k = 2.6 \times 10^9$ dm^3 mol^{-1} s^{-1}, this work; the reasons for this discrepancy are discussed below) governs the chemistry. At high maleimide concentrations, it becomes apparent that the time profiles are not identical at all wavelengths. At shorter wavelengths, the increase in signal intensity follows the laser (double) pulse shape, while above 350 nm the shape of the increase is rounded, that is, delayed (Figure 11). The decay is also somewhat slower.

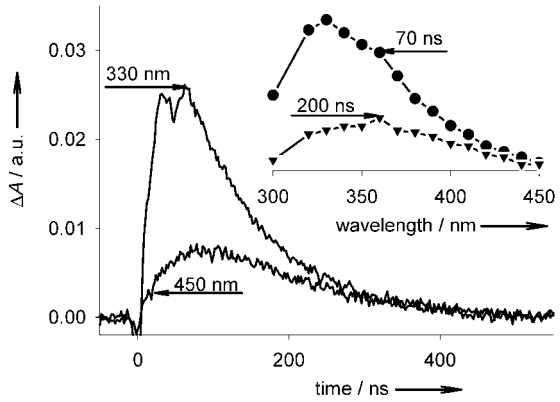

Figure 11. Time profiles and transient spectra (inset) for the self-quenching reaction of maleimide (5.24 mmol dm^{-3}) in acetonitrile, helium purged. The wavelength region below 300 nm is obscured by the high maleimide concentration.

This behaviour is typical for a product that decays faster than it is formed. The effect is more pronounced at longer wavelengths, which means that the spectrum of the product is red-shifted relative to its precursor (Figure 11, inset). This behaviour is also found in the case of *N*-methyl- and *N*-ethylmaleimide, that is, it is not specific to the unsubstituted maleimide.

Aqueous solutions at low pH: At pH 1, at which the deprotonation is efficiently suppressed, the behaviour of the maleimide triplet state corresponds to that in non-aqueous environments.

One product of the reaction of triplet maleimides with ground-state maleimides (self-quenching) is the radical anion **3** (in this case in its protonated form **4** {pH 1 < pK_a(**4**) = 2.85}[8]). The radical cation **7** must also be produced. It probably deprotonates rapidly to yield **11** and thereby escapes detection.[5] The spectrum and the lifetime of the maleimide radical anion **3** and its protonated form **4** differ quite substantially from the short-lived transient that we are concerned with here.

This short-lived transient is produced by first-order kinetics in a reaction with maleimide and then decays rapidly. An increase in the maleimide concentration also increases the temporary concentration of this transient. Spectroscopic reasons limit the maximum applicable maleimide concentration to ≈0.01 mol dm^{-3}.[21] Under these conditions, however, the transient does not yet completely dominate the spectrum. This requires statistical analysis of the entire data set, the so-called "global analysis". Statistical analysis demands the a priori formulation of a mechanism. We found that a simple **A** → **B** → **C** mechanism is sufficient to explain all data (Figure 12).[31] The spectrum of **A** is identical to the initial

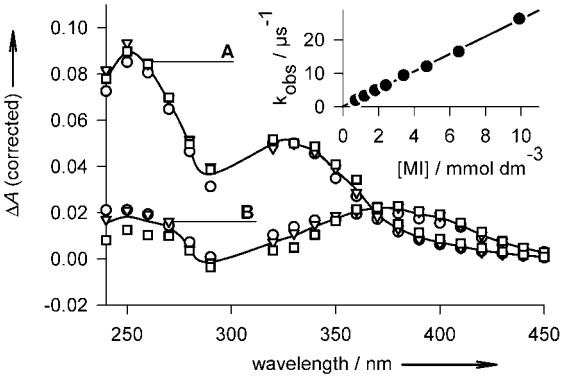

Figure 12. Spectra extracted numerically from flash photolysis data. Self-quenching of triplet maleimide by ground state maleimide. Three runs with different maleimide concentrations are shown in the main graph, (circles, squares and triangles) corrected with the actinometry function.[21] Inset: plot of the observed rate of the first step vs. maleimide concentration with the rate of the subsequent reaction **B** → **C** locked to $k_{B\rightarrow C} = 8 \times 10^6$ s^{-1}. The slope corresponds to a rate of $k_{A\rightarrow B} = 2.6 \times 10^9$ dm^3 mol^{-1} s^{-1}. The intercept lies at 0.2×10^6 s^{-1}, corresponding to an intrinsic triplet lifetime of 5 μs.

spectrum that is always encountered and which is assigned to that of the keto form of the maleimide triplet-state **1**. The spectrum of **B** was found to be identical in shape and absorbance relative to **A** and independent of maleimide concentration. Species **B** was also found to have the same lifetime within tight limits ($\tau = 110$ ns). The total yield of **A** decreases with decreasing ground-state absorbance and was normalised by using the actinometry function.[21]

The intrinsic decay of **A**, which is described by the intercept in the inset of Figure 12, is 0.2×10^6 s^{-1}, and is the same as the value that was obtained from time-resolved conductometry. The reason why we had previously obtained a much faster rate for the intrinsic triplet decay[5] is that the apparent rate of triplet decay is distorted by the dimer triplet with increasing maleimide concentrations. This led to a lower rate of self-quenching and, hence, increased the extrapolated intercept.

The appearance of spectrum **B** is surprising as it does not at all agree in shape and lifetime with the product of self-quenching that was identified earlier (the radical anion **3**).[5] Its rate of formation increases linearly with maleimide

  0947-6539/02/0818-4205 $ 20.00+.50/0

concentration. The transient **B** does not appear when triplet-state maleimides are treated with other electron-donating quenchers in which the maleimide radical anion has also been identified as a product.[5]

For these reasons, the spectrum **B** is assigned to the (short-lived) triplet state of the maleimide cyclobutane dimer **8**. The corresponding ground state **9** is transparent in the region of monitoring and, therefore, escapes detection. Yet, GC-MS analysis has established **9** as a final product (see Experimental Section and Scheme 6)

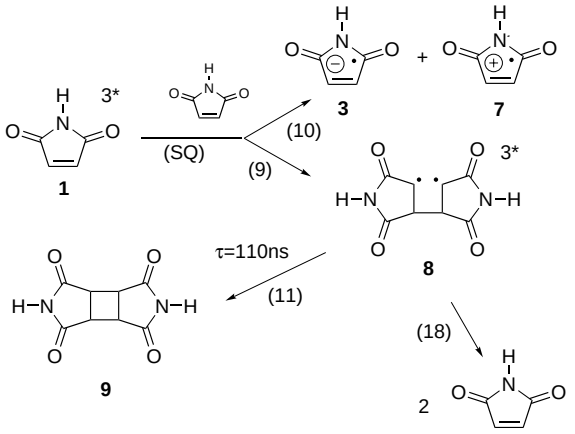

Scheme 6.

Maleimide cyclobutane dimers have already been reported,[9] but without flash photolysis experiments. Put and De Schryver[9] concluded from the relative quantum yields of triplet state and cyclobutane dimer formation that "there is no additional deactivation after addition of the triplet to a ground-state molecule". The product of addition of a triplet-state to a ground-state molecule must, however, retain the triplet multiplicity for a finite time. The lifetime of 110 ns found here (their experimental conditions,[9] dichloromethane at 30 °C, would probably lead to even shorter lifetimes than those observed here) is within the frame of their calculations of "no additional deactivation".

It is important to stress that the evidence for cyclobutane dimer formation does not disprove the formation of radical ions by a concomitant electron-transfer reaction. Indeed, the spectrum of **C** (not shown), although weak and, therefore, noisy, has a maximum around 275 nm as does that of the protonated maleimide radical anion **4**. The spectrum of **B** matches the spectrum of the maleimide hydrogen adduct **2** (Figure 13). This spectrum can be produced independently by two methods: addition of hydrogen atoms which are produced by pulse radiolysis of aqueous maleimide solutions or by the reaction of triplet maleimide with 2-propanol (Figure 11). The hydrogen, alkyl and hydroxyl adduct radicals are not distinguishable by their spectra.[8] The dimer triplet **8** contains the "adduct chromophore" twice. This simple approach, which is supported by the quantum chemical calculations from Table 2, suggests that the dimer-triplet **8** exhibits twice the oscillator strength, that is, twice the absorption coefficient. From the

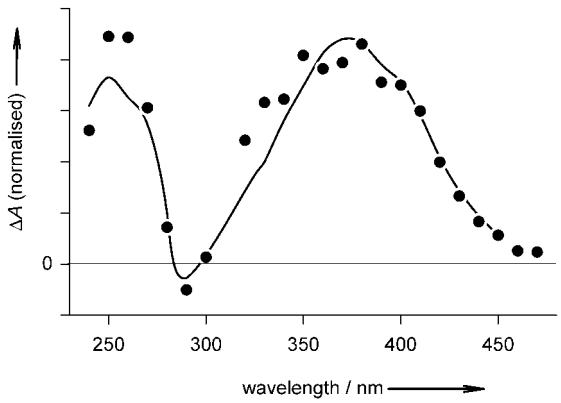

Figure 13. Comparison of the transient spectra of the maleimide-hydrogen adduct (●: maleimide (2.12 mmol dm^{-3}) in helium-purged 2-propanol, flash photolysed, normalised to same height as the solid line (——) of spectrum **B**) and **B** (from Figure 10, ——, attributed to the dimer triplet). Note that the "bleaching" at 290 nm is observed in both cases.

maleimide triplet absorption coefficient,[12] the absorption coefficient of the hydrogen adduct from pulse radiolysis (cf. Experimental Section) and the relative absorbance of **A** and **B**, a dimer triplet **8** yield of 51 ± 10 % is calculated. Put and De Schryver obtained a dimer yield of 25 % relative to the triplet quantum yield with *N*-butylmaleimide in dichloromethane.[9] The difference might be caused by the *N*-substitution, the solvent or by the decay of some of the dimer triplets **8** into two monomers [reaction (18), Scheme 6] rather than into the cyclobutane derivative **9** [reaction (11)].

Implications for photoinitiation

Biradical tetramethylene intermediates (ring-opened cyclobutanes) are commonly proposed as initiating species.[17, 32] Usually, these dimers are supposed to be formed from a donor and an acceptor. We did not find evidence for these heterodimers,[7] but rather for a symmetrical type that arise from two maleimide molecules. In fact, the yield of radical ions increases with increasing electron-donor strength of the reaction partner.[12] Probably the relative importance of electron transfer and cycloaddition depends on the relative donor–acceptor strength of the reaction partners. In this respect maleimides have both electron acceptor and donor properties and undergo cyclobutane formation as well as electron transfer. Schenck and co-workers found high yields of dimers only when maleic anhydride was reacted with electron-deficient olefins, while electron-rich olefins yielded copolymers.[33]

The dimer triplet **8** decays unimolecularly within the concentration range of our experiments (0.7–9.9 mmol dm^{-3}) with the same rate, that is, no further reaction with maleimide was detected. This has also been reported for other maleimides.[9] A rate of 1×10^8 dm^3 mol^{-1} s^{-1} of a reaction of the dimer triplet with maleimide would have led to a 20% increase in dimer triplet decay rate using 10^{-2} mol dm^{-3} maleimide instead of 10^{-3} mol dm^{-3}. An increase of 20% in rate would not have escaped notice. The rate

0947-6539/02/0818-4206 $ 20.00+.50/0 *Chem. Eur. J.* **2002**, *8*, No. 18

of reaction of the dimer triplet with maleimide must therefore be lower than 1×10^8 dm^3 mol^{-1} s^{-1}.

A rate of $< 1 \times 10^8$ dm^3 mol^{-1} s^{-1} can still contribute significantly to initiation. We expect that addition of the dimer triplet **8** to a monomer maleimide is not much faster than propagation. Maleimide propagation is unlikely to be faster than acrylate propagation (10^3–10^4 dm^3 mol^{-1} s^{-1})[34]. In neat maleimide, this would result in a rate $< 10^5$ s^{-1}, which is much smaller than the intrinsic decay of the dimer triplet **8** into **9**, 10^7 s^{-1} ($\tau = 110$ ns). Therefore, the initiation efficiency of the dimer triplet can only be at the most, 1 %. To confirm this, the cyclobutane dimer yield at different *N*-ethylmaleimide concentrations (up to 40 mmol dm^{-3} in acetonitrile) and constant UV dose was determined by GC (maleimide itself is not suitable for GC analysis). The yield is independent of *N*-ethylmaleimide concentration. If its precursor, the dimer triplet, is scavenged by *N*-ethylmaleimide, the cyclobutane dimer yield would decrease with increasing *N*-ethylmaleimide concentration.

For coating purposes, cyclobutane-dimer formation ($\Phi = 0.25$–0.5) is highly undesirable, because it not only consumes photons and photoinitiator, but also produces low molecular-weight migratables (LMWM). Their high yield was not realised when maleimide-photoinitiated resins were proposed as a remedy to LMWM formation.[3]

The radical ion path [reaction (10), Scheme 6, $\approx$10 % yield] yields two transients, the radical anion **3** and cation **7**. The radical anion does not initiate,[28] whereas the radical cation **7**, does.[28] Indeed, all curing experiments with maleimides as photoinitiators that were carried out in this institute had low efficiencies in comparison to conventional photoinitiators.[7]

Conclusion

The photochemistry of maleimides has been shown to include various reaction types: electron transfer, deprotonation, hydrogen abstraction and cyclobutane dimer formation. The reactions put forward in this paper are summarised in Scheme 1. Three different species have been suggested to cause the photoinitiation by maleimides and similar systems, that is, dimer triplets, radical ions, and radicals generated by hydrogen abstraction.

The present paper has now shown that dimer triplets and radical ions are formed concomitantly and evidence is given that dimer triplets are not actively involved in initiation. Hydrogen abstraction occurs when triplet maleimides are exposed to suitable hydrogen donors (e.g., alcohols), but does not play a significant role in neat resins.[5] The maleimide radical anion does not react with olefins.[28] There only remains the radical cation as initiating species, and indeed it was found to give rise to propagating radicals, that is, it was found to initiate.[28]

Maleimides were considered for use as photoinitiators because they form radicals with very high rates.[4] The portion of the maleimide which is not consumed by the photoreaction copolymerises with the usual radiation-curable monomers (i.e., acrylates and vinyl ethers), leading to high-quality transparent and heat resistant materials.[35] However, maleimides exhibit low quantum yields[12] and produce large amounts of by-products. Their high costs and especially their toxicity[36] limit, in the end, their use in practical applications.

Experimental Section

Materials: Maleimide (HMI, 98 + %, Lancaster), *N*-ethylmaleimide (EtMI, 98 + %, Lancaster), 2-nitrobenzaldehyde (ONBA, 99 + %, Lancaster), benzophenone-4-carboxylic acid (4BC, 99 +, Lancaster), potassium fluoride (99.5 %, Fluka), sodium dihydrogen phosphate monohydrate (99 + %, Merck), di-sodium hydrogen phosphate anhydrous (99 + %, Merck), sodium hydroxide (50 % aqueous solution, Baker) and perchloric acid (60 % aqueous solution, Aldrich) were used as received. Water was purified with a Millipore Milli-Q system, and acetonitrile was obtained from Riedel–De Haën (gradient grade). To remove oxygen, samples were purged for 7 min with N_2 (5.0, Air Products) or with He (4.6, Linde).

GC, GC-MS: The relative dimer yield (of EtMI) was quantified by GC (HP 5890 II, 15 m Rtx-65TG S-56 column, 50–300 °C at 6 K min^{-1}, retention time 25.5 min). The dimer was identified by its mass spectrum: MW 250: *m*/*z* (%): 250 (100), 235 (21), 151 (63), 125 (82), 108 (38), 80 (62), 52 (56).

Laser flash photolysis: The laser photolysis apparatus was composed of a 308 nm XeCl-excimer laser as excitation source (MINex, LTB Berlin, pulse train of three pulses of 70 %, 20 % and 10 % of total energy, each with 5 ns half width within 70 ns, total pulse train energy up to 15 mJ) and a pulsed xenon short-arc lamp (XBO 450 or 1000, Osram, power supply LPS 1200, lamp pulser MCP 2010, both Photon Technology International), which supplied the analyzing light. The transient recording electronics, a photomultiplier (1P28, Hamamatsu, which was operated at 900 V, power supply: PS 310, Stanford Research Systems) and a 500 MHz, 2.5 GS s^{-1} digitizing storage oscilloscope (TDS 620b, Tektronix) guaranteed a time resolution within the limits set by the excitation pulse. All experiments are carried out in flow-through cuvettes with 5×3 mm^2 cross section. Attenuation of the laser pulse energy was performed either with (stacks of) wire mesh filters (54 % transmission) or glass microscope slides. Laser pulse energy was monitored by a fast photodiode which also supplies the trigger pulse (which was the rising edge of the (first) laser pulse).[20] All time points in this paper are given relative to this pulse. Further details have been published recently.[20, 21]

Some experiments were performed with a similar setup (Laser: Radiant-Dyes RD-EXC-100, max. 100 mJ, 17 ns pulse width at half maximum), described elsewhere.[5]

The conductivity detection system was based on a system developed by Bothe and Janata.[37] It consisted of a custom-made quadratic cross section (5×5 mm^2) quartz flow-through cuvette with glassy carbon electrodes (Ø 3 mm) and a 50 V, 1 ms DC pulse generator (HP 214A, Hewlett Packard). The voltage drop over a 50 Ω resistor was amplified tenfold by a custom made 400 MHz–DC amplifier (on basis of a Burr–Brown OPA 687).

Biphotonic excitation was investigated using the laser flash photolysis setup of Dr. H. Görner, Max-Planck-Institut für Strahlenchemie in Mülheim an der Ruhr (308 nm, Lambda-Physik EMG 210 MSC, 20 ns pulse width, 100 mJ maximum pulse energy). The recording electronics and further details of this setup are described elsewhere.[38]

Actinometry: Optical actinometry was performed with benzophenone-4-carboxylate in alkaline solution (formation of the triplet state with a quantum yield Φ of unity, $\varepsilon(340\text{ nm}) = 880$ m^2 mol^{-1}).[39] The dependence of the transient absorbance yield on the ground state absorbance was modeled as in reference [21].

The conductometric detection system was calibrated with the 2-nitrobenzaldehyde actinometer (formation of 2-nitrosobenzoic acid, $\Phi = 0.5$).[22] The signal is a function of the ground state absorbance and was accounted for by the formulae published in reference [12]

  0947-6539/02/0818-4207 $ 20.00+.50/0

Pulse radiolysis: For pulse radiolysis, an 11 MeV linear accelerator that delivers 100 Gy pulses of 17 ns duration was used. The optical detection system was essentially identical with that of the laser flash photolysis apparatus. Dosimetry was performed with N_2O-saturated 0.1 mol dm^{-3} aqueous KSCN solutions.[40] The maleimide hydrogen-adduct spectrum was determined by pulse radiolysis of a nitrogen-degassed solution of maleimide (0.9 mmol dm^{-3}) in aqueous *tert*-butanol (0.5 mol dm^{-3}) at pH 1.25 ($HClO_4$). The spectrum was identical to that shown in Figure 11; λ_{max} (ε) = 370 nm (130 m^2 mol^{-1}). For comparison: *N*-ethylmaleimide hydrogen adduct:[8], λ_{max} (ε) = 400 nm (120 m^2 mol^{-1}).

Data analysis: Two different computer programs were used to extract physical values from the data collected: PC-Pro K[41] for the so-called "global analysis", that is, the determination of reaction rates using the entire experimental wavelength-time-absorbance tensor at once, TableCurve 2D Version 5[42] for the pK_a-value determination and nonlinear fitting of the saturation functions.

Quantum chemical calculations: Quantum chemical calculations were performed by using the density functional theory (DFT) hybrid B3LYP with 6-31G(d) basis set methods (Gaussian 98W).[43]

Acknowledgements

The authors acknowledge H. Görner for the possibility of conducting experiments at his laboratory at the Max-Planck-Institut für Strahlenchemie in Mülheim an der Ruhr. The helpful discussions with I. Janovský and C. von Sonntag are also acknowledged.

[1] The term "initiate" is used throughout this paper to denote "initiation of a free radical vinyl polymerisation".
[2] H. Aida, I. Takase, T. Nozi, *Makromol. Chem.* **1989**, *190*, 2821 – 2831; H. J. Timpe, *Topics Curr. Chem.* **1990**, *156*, 167 – 197.
[3] S. C. Clark, C. E. Hoyle, S. Jönsson, F. Morel, C. Decker, *Photoinitiation Efficiency of N-Functional Aliphaticmaleimides*, Radtech North America, Chicago, **1997**.
[4] K. Visnawathan, S. Clark, C. Miller, C. E. Hoyle, S. Jönsson, L. Shao, *Polym. Prepr.* **1998**, *39*, 644 – 645.
[5] J. von Sonntag, D. Beckert, W. Knolle, R. Mehnert, *Radiat. Phys. Chem.* **1999**, *55*, 609 – 613.
[6] S. C. Clark, *Photopolymerization and Photophysical Studies of N-Aliphaticmaleimides*, Ph.D. Thesis, University of Southern Mississippi, Hattiesburg, MS, **1998**.
[7] J. von Sonntag, Ph.D. Thesis, University of Leipzig, Leipzig (Germany), **2000**.
[8] E. Hayon, M. Simic, *Radiat. Res.* **1972**, *50*, 464 – 478.
[9] J. Put, F. C. De Schryver, *J. Am. Chem. Soc.* **1973**, *95*, 137 – 145.
[10] P. B. Ayscough, A. J. Elliot, *J. Chem. Soc. Faraday Trans. 1* **1976**, *72*, 791 – 798.
[11] P. B. Ayscough, T. H. English, G. Lambert, *J. Chem. Soc. Faraday Trans. 1* **1977**, *73*, 1302 – 1310.
[12] J. von Sonntag, W. Knolle, *J. Photochem. Photobiol. A* **2000**, *136*, 133 – 139.
[13] J. M. Warman, R. Abellon, H. J. Verhey, J. W. Verhoeven, J. W. Hofstraat, *J. Phys. Chem. B* **1997**, *101*, 4913 – 4916; G. Weidinger, *Neue Photoinitiatoren und photoaktive Polymere*, Ph.D. Thesis, Technical University of Vienna, Vienna (Austria), **1993**.
[14] H. Falk, A. Leodolter, *Monatsh. Chem.* **1978**, *109*, 883 – 897.
[15] G. Kaupp, in *CRC Handbook of Organic Photochemistry and Photobiology* (Eds.: W. M. Horspool, P.-S. Song), CRC, Boca Raton, **1995**, pp. 29 – 49.
[16] G. Schmidt -Naake, M. Drache, K. Leonhardt, *Macromol. Chem. Phys.* **1998**, *199*, 353 – 361; H. Aida, I. Takase, T. Nozi, *Makromol. Chem.* **1989**, *190*, 2821 – 2831; S. Jönsson, K. Viswanathan, C. E. Hoyle, S. C. Clark, C. Miller, F. Morel, C. Decker, *Photoexcited State Acceptor Monomers as Initiators for Free Radical Induced Polymerization*, Radtech Asia, Kuala Lumpur, **1999**; N. G. Gaylord, M. Stolka, A. Takahashi, S. Maiti, *J. Macromol. Sci. Chem* **1971**, *5*, 867 – 881; N. J. Turro, P. Wriede, J. C. Dalton, D. Arnold, A. Glick, *J. Am. Chem. Soc.* **1967**, *89*, 3950 – 3952.
[17] H. K. Hall, A. B. Padias, *Acc. Chem. Res.* **1990**, *23*, 3 – 9; M. A. Williamson, J. D. B. Smith, P. M. Castle, R. N. Kauffman, *J. Polym. Sci. Polym. Chem. Ed.* **1982**, *20*, 1875 – 1884; R. K. Sadhir, J. D. B. Smith, *J. Polym. Sci. A* **1992**, *30*, 589 – 595; M. Rätzsch, *Z. Chem.* **1975**, *15*, 341 – 348; N. G. Gaylord, R. Mehta, K. M. Mishra, M. Nagler, *Polym. Prepr.* **1985**, *26*, 180 – 181; M. Rätzsch, G. Schicht, *Acta Polym.* **1980**, *31*, 419 – 423.
[18] M. Eigen, W. Kruse, G. Maass, L. De Maeyer, *Prog. React. Kinetics* **1964**, *2*, 285 – 318.
[19] P. Vanýsek, in *CRC Handbook of Chemistry and Physics*, 71st ed. (Ed.: D. R. Lide), CRC, Boca Raton, **1991**, pp. 5,96 – 95,99.
[20] J. von Sonntag, W. Knolle, *J. Photochem. Photobiol. A* **2000**, *132*, 25 – 27.
[21] J. von Sonntag, *J. Photochem. Photobiol. A* **1999**, *126*, 1 – 5.
[22] R. G. E. Morales, G. P. Jara, *Limnol. Oceanogr.* **1993**, *38*, 703 – 705.
[23] K. D. Asmus, A. Henglein, M. Ebert, J. P. Keene, *Ber. Bunsen-Ges.* **1964**, *68*, 657 – 663.
[24] At neutral pH any HIM^{3*} produced will deprotonate if not removed by another process, that is, the quantum yield of deprotonation is identical with the triplet quantum yield.
[25] P. Krumbiegel, *Isotopieeffekte*, Akademie-Verlag, Berlin, **1970**.
[26] I. Carmichael, G. L. Hug, *J. Phys. Chem. Ref. Data* **1986**, *15*, 1 – 250.
[27] G. L. Hug, *Optical Spectra of Nonmetallic Inorganic Transient Species in Aqueous Solution*, U.S. Government printing office, Washington, D.C., **1981**.
[28] J. von Sonntag, I. Janovský, S. Naumov, R. Mehnert, *Macromol. Chem. Phys.* **2001**, *202*, 1355 – 1360.
[29] D. R. Lide, *CRC Handbook of Chemistry and Physics*, 71st ed. (Ed.: D. R. Lide), CRC, Boca Raton, **1991**.
[30] J. Lind, X. Shen, T. E. Eriksen, G. Merenyi, L. Eberson, *J. Am. Chem. Soc.* **1991**, *113*, 4629 – 4633.
[31] The ground state maleimide is not included as a reactant here, as it is in great excess, and simplicity of the approach has highest priority in this kind of statistical analyses.
[32] C. Decker, D. Decker, *Polymer* **1997**, *38*, 2229 – 2236; C. Göksel, B. Hacioglu, U. Akbulut, *J. Polym. Sci.* **1997**, *35*, 3735 – 3743; X. Li, G. Chen, S. Li, A. Qin, T. Yu, *Makromol. Chem. Rapid Commun.* **1988**, *9*, 195 – 202; A. Torres, F. Castano, J. M. Alvarino, *Makromol. Chem.* **1978**, *179*, 2653 – 2661; M. C. Cole, M. Bachemin, C. K. Nguyen, K. Viswanathan, C. E. Hoyle, S. Jönsson, H. K. Hall, Jr., *Photoinitiatorless Photopolymerizations Involving Monomers That Form Charge Transfer Complexes*, Radtech, Baltimore, MD, **2000**.
[33] R. Steinmetz, W. Hartmann, G. O. Schenck, *Chem. Ber.* **1965**, *98*, 3854 – 3873.
[34] M. Buback, C. Kowollik, *Macromolecules* **1998**, *31*, 3211 – 3215.
[35] Y. Kita, K. Kishino, K. Nakagawa, *J. Appl. Polym. Sci.* **1997**, *63*, 1055 – 1062; Y. Kita, K. Kishino, K. Nakagawa, *J. Appl. Polym. Sci.* **1997**, *63*, 363 – 368.
[36] N. Pietschmann, personal communication, Leipzig, **2000**.
[37] E. Janata, J. Lilie, M. Martin, *Radiat. Phys. Chem.* **1994**, *43*, 353 – 356; E. Bothe, E. Janata, private communications, **1998**.
[38] A. Griesbeck, H. Görner, *J. Photochem. Photobiol. A* **1999**, *129*, 111 – 119; F. Elisei, G. Favaro, H. Görner, *J. Photochem. Photobiol. A* **1991**, *59*, 243 – 253.
[39] J. K. Hurley, H. Linschitz, A. J. Treinin, *J. Phys. Chem.* **1988**, *92*, 5151 – 5159.
[40] G. V. Buxton, C. R. Stuart, *J. Chem. Soc. Faraday Trans.* **1995**, *91*, 279 – 281.
[41] P. J. King, PC Pro-K: global analysis and simulation package for Windows 95 and Windows NT, Applied Photophysics, Leatherhead (UK), **1996**.
[42] *TableCurve 2D Automated Curve Fitting Software User's Manual*, Jandel Corporation, San Rafael, **1994**.
[43] M. J. Frisch, G. W. Trucks, H. B. Schlegel, G. E. Scuseria, M. A. Robb, J. R. Cheeseman, V. G. Zakrzewski, J. A. Montgomery, R. E. Stratmann, J. C. Burant, S. Dapprich, J. M. Millam, A. D. Daniels, K. N. Kudin, M. C. Strain, O. Farkas, J. Tomasi, V. Barone, M. Cossi, R. Cammi, B. Mennucci, C. Pomelli, C. Adamo, S. Clifford, J. Ochterski,

  0947-6539/02/0818-4208 $ 20.00+.50/0

G. A. Petersson, P. Y. Ayala, Q. Cui, K. Morokuma, D. K. Malick, A. D. Rabuck, K. Raghavachari, J. B. Foresman, J. Cioslowski, J. V. Ortiz, B. B. Stefanov, G. Liu, A. Liashenko, P. Piskorz, I. Komaromi, R. Gomperts, R. L. Martin, D. J. Fox, T. Keith, M. A. Al -Laham, C. Y. Peng, A. Nanayakkara, C. Gonzalez, M. Challacombe, P. M. W. Gill, B. G. Johnson, W. Chen, M. W. Wong, J. L. Andres, M. Head-Gordon, E. S. Replogle, J. A. Pople, *Gaussian 98 (Revision A.9)*, Gaussian Inc., Pittsburgh, PA, **2000**.

Received: January 31, 2002 [F3843]

  0947-6539/02/0818-4209 $ 20.00+.50/0